

# Microvasculature Visualization Using Motion-Corrected non-Contrast-Enhanced Thyroid and Liver Fibrosis Ultrasound Images

Lan Lan;<sup>1</sup> Soroosh Sabeti, PhD;<sup>2</sup> Azra Alizad, MD<sup>3</sup>

<sup>1</sup>Department of Biomedical Engineering, Georgia Institute of Technology; <sup>2</sup>Department of Physiology and Biomedical Engineering, Mayo Clinic College of Medicine and Science; <sup>3</sup>Department of Radiology, Mayo Clinic College of Medicine and Science

## INTRODUCTION

Early stages of liver fibrosis [1] and thyroid malignancy [2] manifest in microvascular structures, which can be visualized with ultrasound imaging. One of the biggest challenges facing liver and thyroid microvasculature imaging is motion artifact originating from physiological motion and the sonographer's hand motion during ultrasound acquisition. The B-Spline, Grid, Image, and Point-Based algorithm has been proven effective for image registration in ultrasound images [3]. This algorithm can estimate affine Transformation from a moving image (I-mov) to a reference image (I-ref) and outputs a displacement matrix that can transform I-ref to I-mov. Affine Transformation in 2D image is described as:

$$T_{affine}(x, y) = \begin{pmatrix} \theta_{11} & \theta_{12} \\ \theta_{21} & \theta_{22} \end{pmatrix} \begin{pmatrix} x \\ y \end{pmatrix} + \begin{pmatrix} \theta_{13} \\ \theta_{23} \end{pmatrix}$$

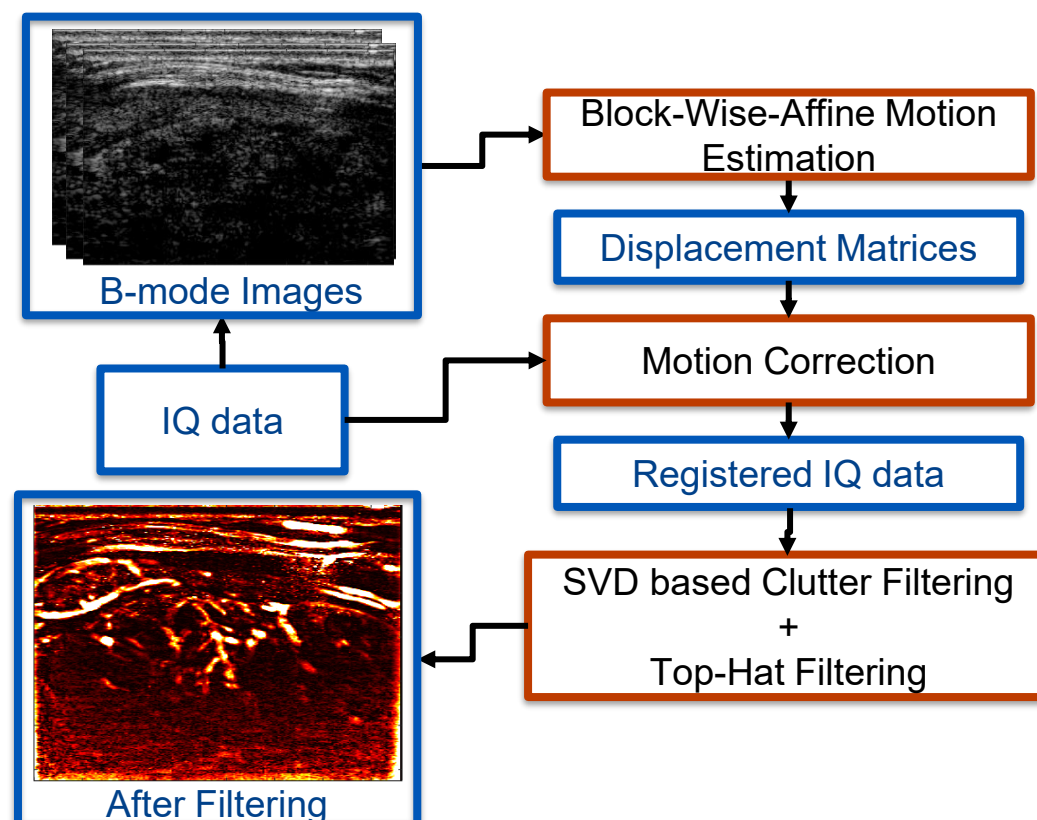
The algorithm optimizes the affine transformation parameters  $\theta$  by maximizing the Normalized Cross-Correlation between I-mov and I-ref via a multiresolution search strategy [4].

## OBJECTIVE

This project aimed to implement the affine image registration algorithm in a block-wise manner for motion estimation on non-contrast-enhanced thyroid and liver fibrosis ultrasound images. The SNR, CNR, and intensity profile at selected ROIs after clutter and Top-Hat filtering were used to evaluate the effectiveness of the algorithm.

## METHODS

Fig 1. Processing Pipeline



### Block-Wise Affine Motion Estimation

The frame with the highest Normalized Cross-Correlation was selected as I-ref, and all the other frames were treated as I-mov. Each pair of I-ref and I-mov were divided into square blocks that were 60 pixels by 60 pixels in size with 75% overlap. The displacement matrix estimated from each block was weighted by a Hamming filter and averaged across overlapping regions to get the total displacement of the entire image.

### Clinical Study

The thyroid and liver ultrasound images were acquired from two male subjects using SC1-4H curvilinear transducer attached to a clinical ultrasound Imaging system (Alpinon E-Cube 12R).

### Processing Pipeline

Affine displacements were estimated from B-mode images extracted from the raw IQ data, and registration was applied to the raw IQ data. Singular-Value-Decomposition-based clutter filtering was applied to the registered IQ data to suppress tissue signals, and Top-Hat filtering was used to remove background noise. A diagram of the pipeline was shown in Figure 1.

## RESULTS – THYROID

Fig 2. Original Thyroid Vessels

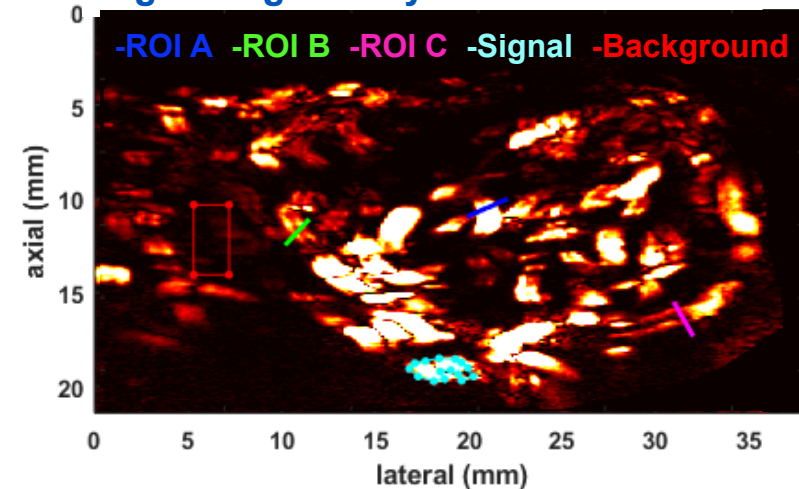


Fig 4. Intensity Profile at ROI A

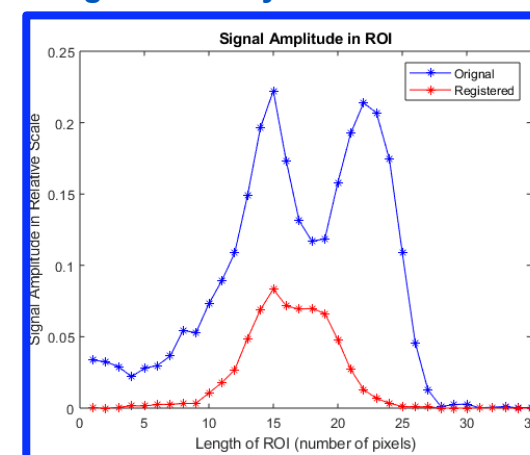


Fig 5. Intensity Profile at ROI B

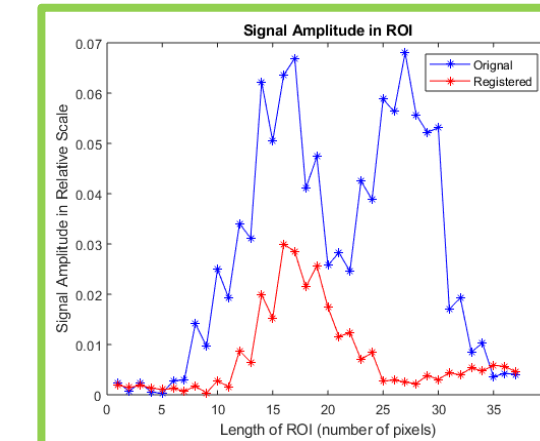


Fig 3. Registered Thyroid Vessels

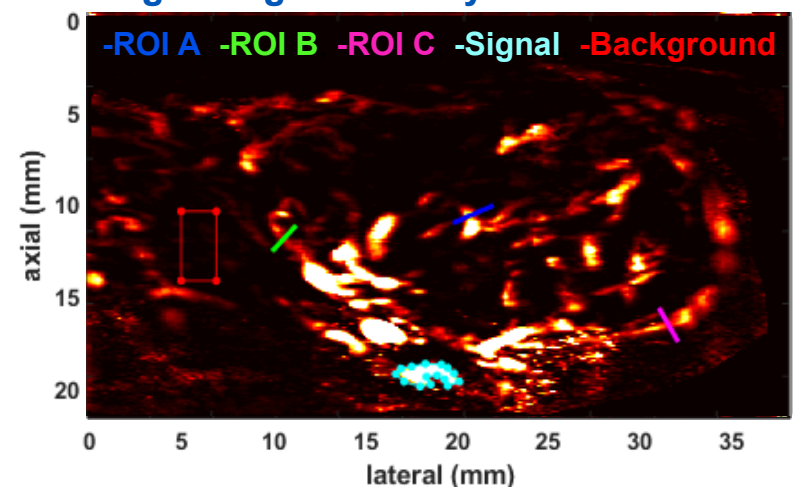


Fig 6. Intensity Profile at ROI C

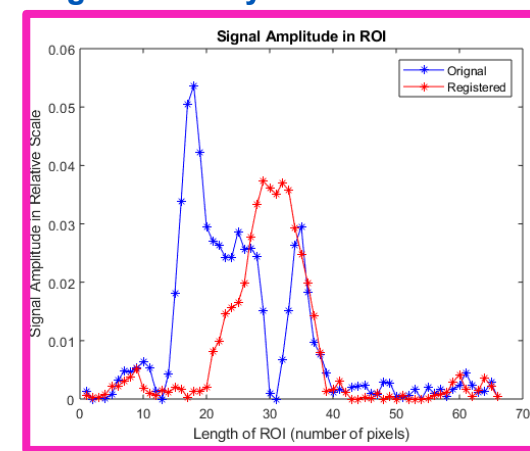
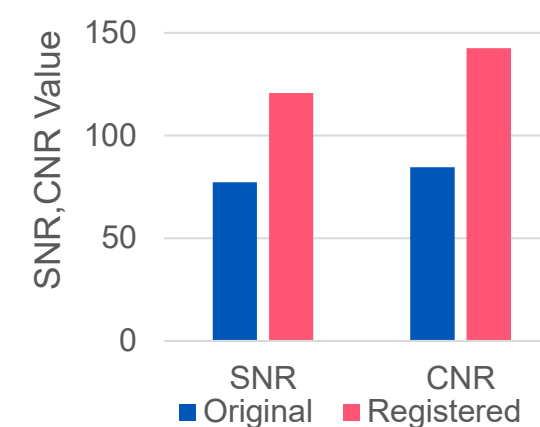


Fig 7. SNR, CNR before and after Motion-Correction



## RESULTS – LIVER FIBROSIS

Fig 8. Original Liver Vessels

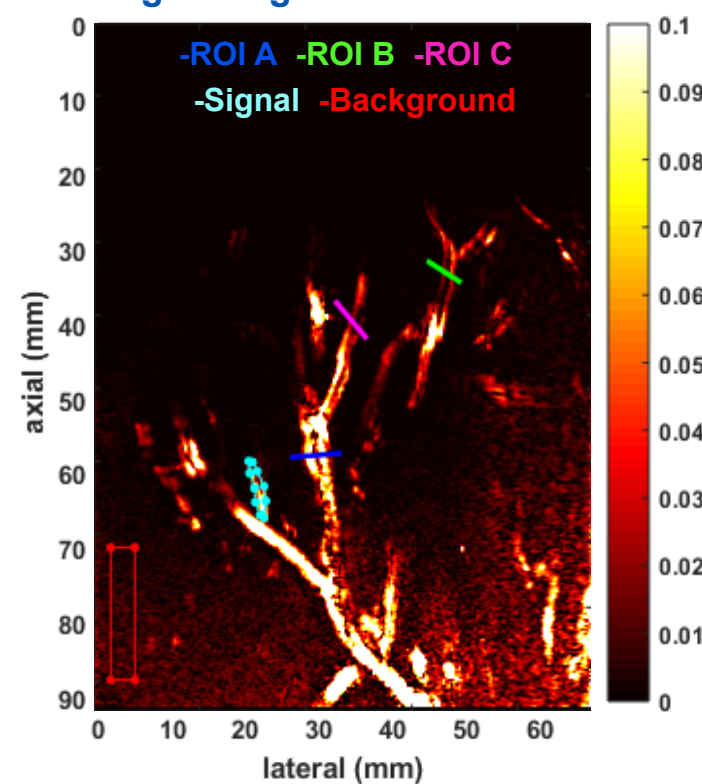


Fig 9. Registered Liver Vessels

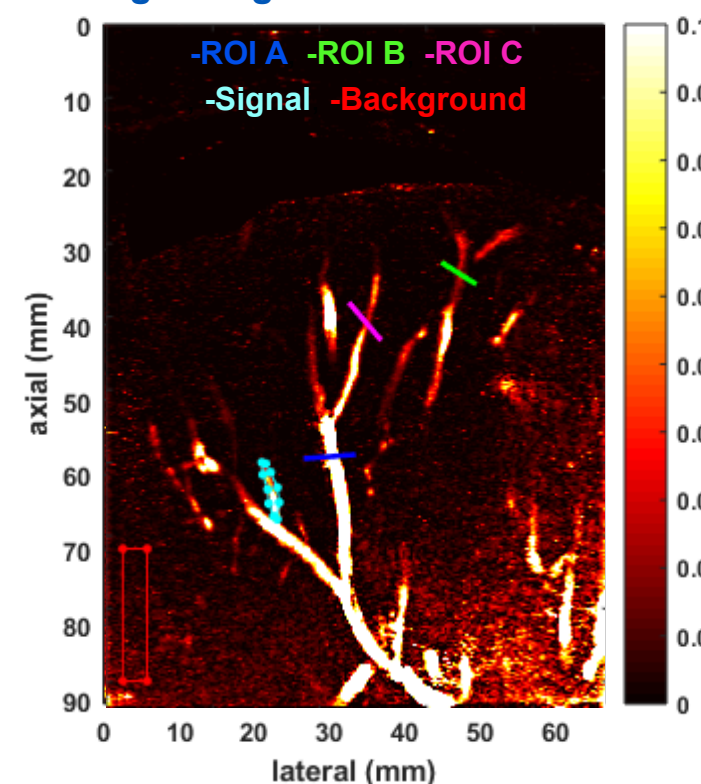


Fig 10. Intensity Profile at ROI A

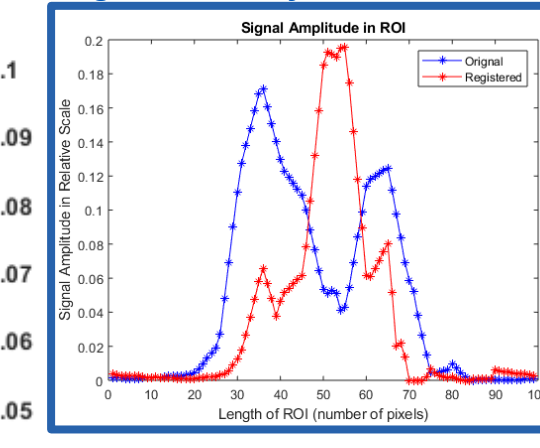


Fig 11. Intensity Profile at ROI B

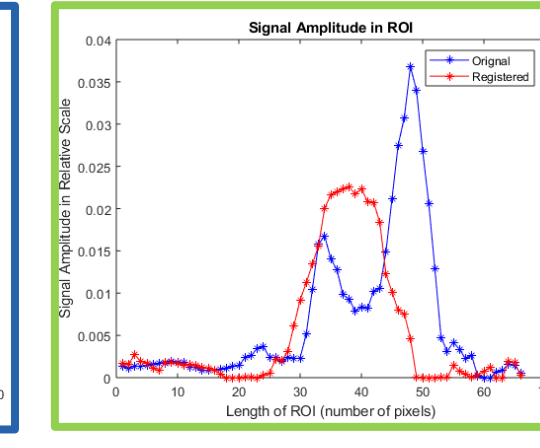


Fig 12. Intensity Profile at ROI C

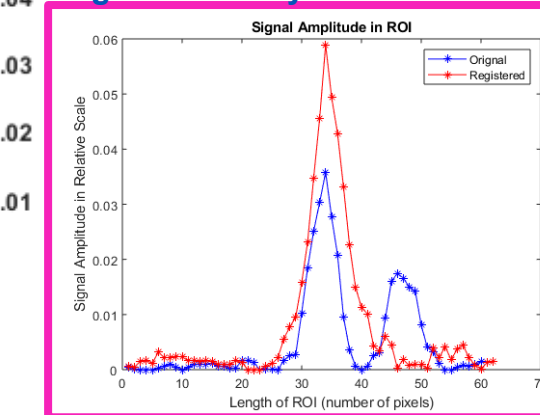
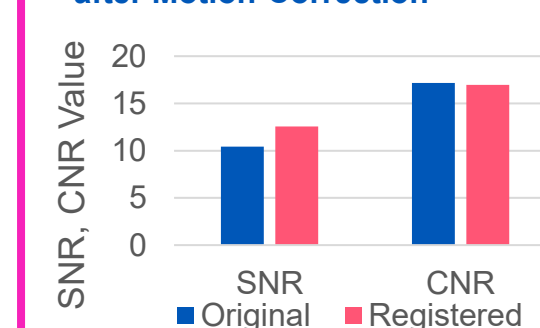


Fig 13. SNR, CNR before and after Motion-Correction



## DISCUSSION

### Thyroid Results

The original image of thyroid vessels experienced severe blurring artifacts (Fig. 2). After registration, these artifacts were attenuated (Fig. 3); as shown in the intensity profiles at ROI A-C (Fig. 4-5), the registration reduced the blurring artifacts from 2 peaks to 1 peak. However, the amplitude of the registered signal did not increase in ROI A and B. In addition, few introduced salt-and-pepper noise was observed at the bottom of the registered image. Nevertheless, CNR and SNR increased after registration (Fig. 7), suggesting that the registered image gives a cleaner background overall, although the signal amplitude might not increase in all regions.

### Liver Fibrosis Results

The original image of the liver vessels also experienced severe blurring artifacts (Fig 8), and those artifacts were compensated after registration (Fig 9). From the intensity profiles at ROI A-C (Fig. 10-12), one can observe that the blurring artifacts were reduced from 2 peaks to 1 peak, and the registered signal amplitude also increased in most of the ROIs. However, there seemed to be more introduced salt-and-pepper noise in the registered image. Therefore, despite increasing signal amplitude, the SNR and CNR did not change much after registration (Fig. 13).

## CONCLUSION

- The results demonstrated that the algorithm effectively compensated for motion artifacts but might introduce salt-and-pepper noise.
- The study was done on a small data set; more investigations are needed to evaluate the algorithm's robustness.
- There was no ground truth as data were acquired from in vivo studies, and no phantom study was done.

## ACKNOWLEDGEMENT

Thank you, Dr. Sabeti, Dr. Alizad, and Dr. Fatemi, for supporting this study. NIH grants supported this study: R25-DK101405, R01 CA239548, and R01 HL148664.

## REFERENCES

- Sherman IA, Pappas SC, Fisher MM. Hepatic microvascular changes associated with development of liver fibrosis and cirrhosis. *Am J Physiol*. 1990;258(2 Pt 2):H460-465. doi:10.1152/ajpheart.1990.258.2.H460
- Hong MJ, Ahn HS, Ha SM, Park HJ, Oh J. Quantitative analysis of vascularity for thyroid nodules on ultrasound using superb microvascular imaging: Can nodular vascularity differentiate between malignant and benign thyroid nodules? *Medicine*. 2022;101(5):e28725. doi:10.1097/MD.00000000000028725
- Dirk-Jan Kroon (2022). B-spline Grid, Image and Point based Registration (<https://www.mathworks.com/matlabcentral/fileexchange/20057-b-spline-grid-image-and-point-based-registration>), MATLAB Central File Exchange. Retrieved July 20, 2022.
- D. Rueckert, L. I. Sonoda, C. Hayes, D. L. G. Hill, M. O. Leach and D. J. Hawkes, "Nonrigid registration using free-form deformations: application to breast MR images," in *IEEE Transactions on Medical Imaging*, vol. 18, no. 8, pp. 712-721, Aug. 1999, doi: 10.1109/42.796284.